

# A sensitivity study for full-field inversion of geo-acoustic data with a towed array in shallow water

S. Jesus

UCEH - University of Algarve, PT-8000 Faro, Portugal \*

This paper presents some of the preliminary work aimed at estimating the ocean bottom morphological structure in coastal waters using a towed array. In order to obtain an idea of the expected performance of the system and draw some conclusions on its operation this study presents the sensitivity of three processors to variations of: array length, source and receiver positions, sensor noise, source frequency and frequency band. Conclusions tend to demonstrate that cost function sensitivity to sound speed variations is higher on the bottom top layers and it increases with array length. An increased sensitivity is generally accompanied by a cost function non-monotonic behavior creating local minima and making it more difficult to reach the global minimum. Attenuations have in general small influence on the acoustic field structure and are therefore difficult to estimate. Increasing the signal frequency band by incoherent module averaging has no significant influence on sensitivity. A cost function relying on the conventional matched filter has shown low sensitivity to sensor noise and is being extended to matching directional data from bottom arrivals at several frequencies. Mismatch cases, mainly those related to array/source relative position, will be also presented.

## 1. INTRODUCTION

Geo-acoustic full-field inversion techniques aim at estimating environmental parameters using the sea-bottom reflected energy received at an array of acoustic sensors. As the received acoustic field is a highly non-linear multi-parameter function of the environmental parameters, direct inversion is useless and one has to resort to inversion by repetitive forward modeling. Matched-field processing is a well known approach that explores a previously defined parameter space and computes the spatial correlation between the predicted acoustic field and the array measured field. Thus, the maximum of the obtained figure of merit is an estimate of the desired parameter. This approach has been widely used for source localization under a variety of environments [1-3] and for a number of different processors [4-5]. When dealing with environmental parameters, and in particu-

---

\*This research was supported by the MAST 2 program of the European Community under contract MAS2-CT920022.

lar for geo-acoustic parameters, the parameter search space is so large that an extensive exploration would be computer time prohibitive. To that end, sophisticated search algorithms have been employed in order to minimize computation time [6-7]. A common requirement to those algorithms is the definition of the cost function to be minimized that compares the predicted and the measured acoustic fields. A number of cost functions have been proposed in the literature that use different data types: transmission loss data, complex acoustic pressure, complex or real wavenumber space spectra, reflection data, etc... Each of these data types has its own processing requirements and represent different amounts of information yielding therefore different results. This study concentrates on the data reduction processing to be performed before minimization and uses as criteria of performance the regularity (number of maxima) and sensitivity of the cost function to the variation of the environmental parameters under estimation. The simulation test case uses a moderate aperture horizontal receiving array and a sound source being towed by a single ship such that the source-receiver range is constant.

## 2. THEORY

### 2.1. Background

The solution to the wave equation for an harmonic source exciting a range-independent environment expressed in the horizontal wavenumber domain is well-known to be the depth-dependent Green's function from which the range dependent solution can be derived using an inverse zero-order Hankel transform. Under the long range approximation (plane-wave assumption) the direct Hankel transform can be evaluated as

$$g(k) = \frac{e^{i\pi/4}}{\sqrt{2\pi k}} \int_0^\infty \phi(r) e^{-ikr} \sqrt{r} dr \quad (1)$$

that is commonly implemented using a Fourier transform under its fast discrete FFT form. Eq. (1) expresses a relationship between the wavenumber field  $g(k)$  and the spatial acoustic pressure  $\phi(r)$ , that is to say, that  $|g(k)|^2$  represents the power received along wavenumber (or direction)  $\vec{k}$  and can be viewed as equivalent to the output of a conventional delay-sum beamformer.

### 2.2. The data model

The received signal is modeled as the wave equation's solution (1) at the receiver location for a narrowband point source exciting a horizontally stratified range independent medium. The normalized spatial dependence of the acoustic pressure field measured at the  $l$ th sensor location  $\theta_l = (r_l, z_l)$  where  $r_l$  and  $z_l$  are the  $l$ th sensor depth and range respectively, due to a unit power harmonic source at frequency  $\omega$  and depth  $z_0$  can be expressed as

$$p_l(\omega; \theta_l, \gamma, z_0) = \int_0^\infty g(k, \omega; \theta_l, \gamma, z_0) J_0(kr_l) k dk, \quad (2)$$

where  $\gamma$  is a vector containing the environmental parameters describing the propagation medium. For clarity, the indexes  $\theta$  and  $z_0$  will be generally omitted and will be introduced

only when necessary for understanding. Let

$$\mathbf{y}_n(\omega_k, \gamma_T) = b_n(\omega_k)\mathbf{p}(\omega_k, \gamma_T) + \boldsymbol{\epsilon}_n(\omega_k), \quad n = 1, \dots, N; k = 1, \dots, K, \quad (3)$$

be the  $L$ -dimensional array of received acoustic pressure at a discrete frequency  $\omega_k$  modeled, for a given  $k$ , as an  $N$  sample draw of a multivariate, complex, normally distributed random variable  $Y$ ,  $N(\mathbf{0}, \mathbf{R}_y)$  where the signal in Eq. (3) is assumed to be corrupted by additive, uncorrelated and zero-mean complex Gaussian noise  $\boldsymbol{\epsilon}_n$  and where  $b_n(\omega_k)$  is a complex random variable that represents the source amplitude at frequency  $\omega_k$  and time snapshot  $n$ . The quantity  $\gamma_T$  is, in that case, the true value of the environmental parameter vector  $\gamma$ .

### 2.3. The matched-field processors

1. The *conventional full-field matched filter* is given by

$$\Phi_{\text{CMF}}(\omega_k, \gamma) = \mathbf{p}(\omega_k, \gamma)^H \hat{\mathbf{R}}_y(\omega_k) \mathbf{p}(\omega_k, \gamma), \quad \gamma \in \Gamma \quad (4)$$

where  $\Gamma$  is the  $M$ -dimensional environmental parameter search space and  $\hat{\mathbf{R}}_y(\omega_k)$  is the sample cross-covariance matrix of the received signal, commonly estimated as the  $N$  sample-mean of the received data outer product.

2. Another possible cost function is the classical *mean square error* function

$$\Phi_{\text{MSE}}(\omega_k, \gamma) = \sum_{l=1}^L [|y_l(\omega_k, \gamma_T)| - |p_l(\omega_k, \gamma)|]^2. \quad (5)$$

That expression is insensitive to differences on signal phase which is certainly a disadvantage, when compared to (4), if the phase is correctly estimated. However, if there are errors on the measurement of signal phase the use of (5) might turn out to give better results

3. The *correlation of wavenumber space spectra* answers to a common problem encountered when analysing geo-acoustic data that is the superposition of the direct path source arrival with the bottom reflected data of interest. A possibility for separating those arrivals is by analysing the data in the wavenumber space domain and filter out the direct path arrivals. For an horizontal array the arrivals associated with the steepest vertical angles, which are those that have a stronger interaction with the bottom, correspond to those arriving closer to broadside. In practice, since the acoustic pressure is a discrete function defined over a finite array aperture, it implies that an estimate of the predicted Green's function can be given by a discrete representation of (1), denoted  $\hat{g}_p(k_j, \omega, \gamma)$ , where the discretization over the wavenumber space has been done arbitrarily over  $N_w$  equally spaced points in  $[0, 2\pi/d]$ ,  $d$  being the array sensor spacing (assumed constant). A one-to-one mapping from the wavenumber to the bearing space may be performed using  $k_j = (2\pi f/c) \cos(\theta_j + \pi/2)$  for  $\theta_j \in [-90^\circ, +90^\circ]$ . With that definition  $-90^\circ$  direction is aft (towards the source) and  $+90^\circ$  is end fire. A similar operation may be performed for the received data vector yielding the wavenumber space observation

$\hat{g}_y(k_j, \omega, \gamma_T)$ . Once a given bearing sector  $\theta_j \in [\theta_l, \theta_h]$  has been selected a possible cost function can be build as

$$\Phi_{\text{WS-CMF}}(\omega_k, \gamma) = \left| \sum_{j=j_l}^{j_h} \hat{g}_y^*(\theta_j, \omega_k, \gamma_T) \hat{g}_p(\theta_j, \omega_k, \gamma) \right|^2 \quad (6)$$

For each of those three processors multiple frequency combination may be obtained by inchoerent averaging of a series of estimates at each single frequency over the band, such that,

$$\Phi_{(\bullet)}(\gamma) = \frac{1}{k_h - k_l + 1} \sum_{k=k_l}^{k_h} \Phi_{(\bullet)}(\omega_k, \gamma) \quad (7)$$

Full-field inversion can be implemented using either (4-6) or their broadband couterpart (7) as cost function. Eq. (7) has, in principle, the advantage of being able to include the amount of information received over a given frequency band and therefore combine a higher sediment penetration at lower frequencies with a higher resolution at higher frequencies into a single estimator.

### 3. SIMULATION RESULTS

Depth (m)	P vel. (m/s)	S vel. (m/s)	P att. (dB/ $\lambda$ )	S att. (dB/ $\lambda$ )	Dens. (g/cm <sup>3</sup> )
0.0	1500	0.0	0.0	0.0	1
140	1550	130	0.1	1.7	1.49
145	1700	350	0.8	2.0	1.88
150	2500	900	0.01	0.01	2.4

Table 1: environmental parameters

The environment parameters are shown on table 1. The system parameters are as follows: the array is composed of 64 hydrophones at 4 m spacing, the source frequency is 100 Hz, the array and source depths are both equal to 100 m, the source-receiver range is 200 m and SNR is infinity. The sensitivity study for those system parameters implies a relatively large number of curves that can not be shown here. The results that have been obtained will be stressed and commented and only a couple of typical examples will be illustrated.

- *Array length:* an increase of array aperture results in a better discrimination of spatial features leading to a higher sensitivity to bottom parameters both in terms of compressional and speed and attenuation. Shear parameters are relatively insensitive to array aperture, at least for this case and at this frequency.
- *Source frequency:* a change of signal frequency between 25 and 200 Hz does change the signal wavelength and thus the angle of incidence at the bottom interface. As

it may be expected, higher frequencies provided better resolution at the top layers and their influence decreased with depth into the bottom. Lower frequencies had the advantage of improving estimate quality of shear parameters at deeper layers. For inversion purpose an optimal frequency interval could be 75-100 Hz providing the overall highest sensitivity and smoothest curves.

- *Bandwidth:* eq.(7) has been used with bandwidths from 10 to 60 Hz corresponding to approximately 3 to 16 averaged frequency bins. One could expect a linear increase of sensitivity with increasing bandwidth. This is not the case since only a slight amelioration has been noticed from a single bin to the 10 Hz case. However the curve smoothness is higher with larger bandwidths which might be a non negligible advantage when using minima based search algorithms for inversion that tend to be seriously degraded by extremely “peaky” cost-functions. This behaviour is similar to that encountered on matched-field processing for source localization [4] where broadband processing provided a smoother background and only a slight increase on peak-to-sidelobe ratio.

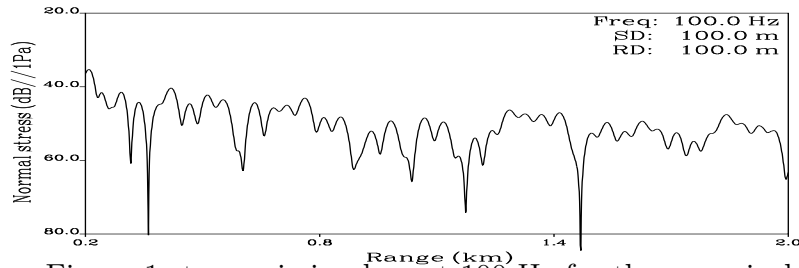


Figure 1: transmission loss at 100 Hz for the canonical case

- *Source-receiver position:* the variation of source-receiver relative depths gave, as expected, variable results depending on the modal distribution over the water column. In terms of source-receiver range a maximum sensitivity on all layers has been obtained at 400 m which in that case coincides with a position of the 252 m long array positioned between the two deep nulls of the transmission loss curve as shown on figure 1. Moreover these two deep nulls are due to the periodic interference pattern of the lower order modes that, for our purpose, do not carry significant information since they do not interact significantly with the bottom.
- *System parameters mismatch:* mismatch appears when the measured and the replica fields are computed using different system configurations. Range and depth mismatches between  $1/15$  and  $1$  wavelength showed that errors larger than  $1/5$  wavelength in depth and  $1/2$  wavelength in range completely destroyed the match. Shear parameters showed a higher sensitivity than compressional parameters to mismatch.
- *Signal-to-noise ratio:* the three processors (4-6) have been used with SNR from -5 to 20 dB. For the wavenumber-space processor (6) the wavenumber “look” window used was  $k_j \in [0.2, 0.45]$  which represents most of the energy of the discrete mode spectrum propagating in the waveguide. The most sensitive cost function at high SNR is, as expected, the MLS processor given by (5). When decreasing SNR the

MLS cost function becomes very erratic and biased while the CMF and WS processors continue to give very consistent results until 0 dB. Further testing is needed in order to determine the behaviour of the WS processor when decreasing and/or moving the wavenumber space “look” window. Due to the “large” window used in this example the CMF and WS processors gave similar results.

#### 4. CONCLUSION

The present study concentrated on the cost function system dependence and on its operational characterization. Conclusions tend to demonstrate that cost function sensitivity to sound speed variations is higher on the bottom top layers and it increases with array length. An increased sensitivity is generally accompanied by a cost function non-monotonic behavior creating local minima and making it hazardous to reach the global minimum. Density and attenuations (both compressional and shear) have in general small influence on the acoustic field structure and are therefore difficult to estimate. Increasing the signal frequency bandwidth by incoherent module averaging has no significant influence on sensitivity. A cost function relying on the conventional matched filter has shown low sensitivity to sensor noise and when used to coherently match directional data from bottom arrivals has shown superior results than the other processors. Mismatch cases, mainly those related to array/source relative position, showed that deviations of more than  $\lambda/2$  in range and  $\lambda/5$  in depth may give erroneous extremum location and therefore biased final estimates.

#### REFERENCES

1. H.P. Bucker, Use of calculated sound fields and matched-field detection to locate sound sources in shallow water, *J. Acoust. Soc. Am.* **59**, 368-373 (1976).
2. T.C. Yang, A method of range and depth estimation by modal decomposition, *J. Acoust. Soc. Am.* **83** 1736-1745 (1988)
3. J.Q.D. Tran and W.S. Hodgkiss, Matched-field processing of a 200 Hz continuous wave (cw) signals, *J. Acoust. Soc. Am.* **89** 745-755 (1991).
4. S.M. Jesus, Broadband matched-field processing of transient signals in shallow water, *J. Acoust. Soc. Am.* **93**(4), Pt.1, 1841-1850 (1993).
5. G.B. Smith, C. Feuillade, D.R. Del Balzo and C.L. Byrne, A non-linear matched-field processor for detection and localization of a quiet source in a noisy shallow water environment, *J. Acoust. Soc. Am.* **85**, 1158-1166, (1989).
6. Michael D. Collins and W.A. Kuperman, Nonlinear inversion for ocean-bottom properties, *J. Acoust. Soc. Am.* **92** (5), 2770-2783, (1992).
7. A. Turgut, Simulated annealing and genetic algorithms in shear modulus inversion of shallow-water sediments, *J. Acoust. Soc. Am.* **93**, (4) Pt.2, 2aAO15, (1993).